Analysis of Current Resonances due to Winding Parasitic Capacitances in Medium-Voltage Medium-Frequency Transformers

Roderick Amir Gomez Jimenez[†], Germán G. Oggier[‡], David Porras[†], and Juan Carlos Balda[†]

[†] Department of Electrical Engineering, University of Arkansas, Fayetteville Arkansas, USA.
[‡]Grupo de Electrónica Aplicada (GEA)/Instituto de Investigaciones en Tecnologías Energéticas y Materiales Avanzados (IITEMA)
Universidad Nacional de Río Cuarto (UNRC), CONICET, Río Cuarto Córdoba, Argentina.
ragomezj@uark.edu, goggier@ieee.org, daporras@uark.edu and jbalda@uark.edu

***Abstract*—This paper presents the analysis of the current resonances on medium-voltage, medium-frequency transformers due to the parasitic capacitances of the windings. Converter performance is affected by these high-frequency current resonances; therefore, the winding arrangement of high-voltage high-turns ratio transformers must be carefully considered during the building process. Three different windings arrangements are built for a 5-kV-to-400-V, 10-kHz transformer for a high-power dual-active-bridge (DAB) converter. Open-circuit and short-circuit impedance response of the three windings are compared. Experimental results include open-circuit test on each of the three different winding arrangements and a 10 kW load test to illustrate the effect of the parasitic capacitances.**

***Index Terms*—Nanocrystalline transformer, medium-frequency transformer (MFT), current resonant, high-voltage transformer,fold-back winding, solid-state transformer (SST).**

I. Introduction

The dual active bridge converter (DAB) is one of the most promising isolated DC/DC converters to meet grid high efficiency and flexibility requirements for future power systems [1]–[3]. This converter presents the advantages of galvanic isolation, bidirectional power flow, simple control strategy, a wide range of input and output voltages, operation with high frequency and power density, making it a promising solution for high power density applications. Some examples include grid connection of renewable energy sources and storage systems [4], [5], EV fast chargers [6], etc.

Despised these advantages, the high-frequency transformer on the DAB faces the challenge of meeting the low leakage and high-efficiency requirements; including, low parasitic capacitances to avoid current resonances [7], [8]. This last requirement is particularly important because one of the effects of these parasitic capacitances includes low-frequency current resonances that can greatly affect the overall efficiency of the converter, this specially affects soft-switching topologies that depends on LC resonant tanks that can be affected by harmonic distortions which leads to hard-switching behavior and a drop in the efficiency [7]–[12]. In medium-frequency and specially in medium-voltage transformers, these effects need to be carefully studied since leakage inductance and stray capacitances have a major effect in the full characterization of the transformer, and these parasitic capacitance is high in high-voltage applications due to the number of turns to achieve a high-step-up ratio [13]. These effects are normally not present in the conventional model of the transformers and a more complete model that truly represents its behavior over a wide range of frequencies is needed [13]–[15].

The main objective of this paper is to analyze the impact of the parasitic capacitances on high-turns ratio high-voltage transformers and explore their mitigation using different winding arrangements. To study the impact of these stray capacitances on the converter performance, three different windings arrangements are built for a 5-kV-to-400-V, 10-kHz high power transformer. Section II presents the analysis and effects of the parasitic capacitances correlated to the winding configuration of the transformer. Section III presents the measured impedance response of each winding arrangements using a vector network analyzer. Finally, IV shows the experimental characterization of the three windings under no-load conditions and the effect of the parasitic capacitance on the current resonances. Also, experimental results under a 10kW load are presented.

II. Transformer Parasitic Capacitances and winding configuration

Parasitic capacitances of medium-frequency transformers are due to the distributed electrical coupling between any two conductors. These include the winding to core capacitance, the winding to winding capacitance, and the layer to layer capacitance for multi-layer windings [7], [13]. These parasitic capacitances result in current spikes and propagation of conducted EMI, which significantly affect the converter performance [7],

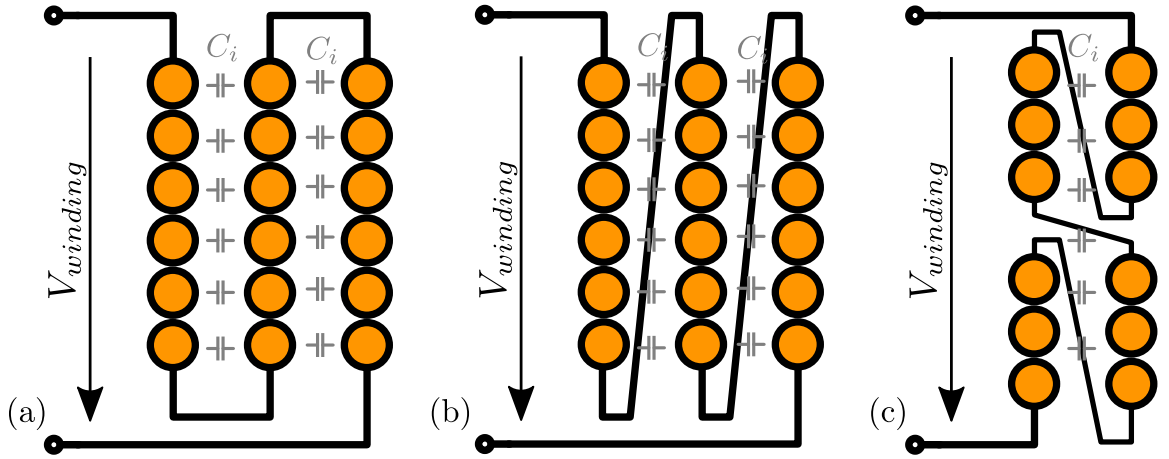

Fig. 1. Considered winding arrangements (a) Conventional multi-layer winding; (b) Fold-back winding; (c) Split fold-back winding.

Fig. 2. Conventional winding arrangement (red) and triple fold-back winding arrangements (black).

TABLE I
TRANSFORMER PROTOTYPE DESIGN PARAMETERS

Parameter	Value
$Input\ Voltage$	5 kV
$Output\ Voltage$	400 V
$Frequency$	10 kHz
$Core\ Type$	$Shell-type$
$Material$	$Nanocrystalline$
$Primary\ Winding$	$Litz\ wire\ \varnothing\ 0.2mm,\ 45\ turns$
$Secondary\ Winding$	$Litz\ wire\ \varnothing\ 0.2mm,\ 6\ turns$

[8], [10], [16], [17]. Consequently, substantial attention has been drawn to the mitigation of the winding capacitance.

The winding capacitance can be analyzed by using the energy-base approach since the induced voltages in all the turns are identical [7], [18]. The electrostatic energy stored in the transformer is given in 1.

$$W = \frac{C_i}{2}\left(\frac{V_1^2}{3} + \frac{V_2^2}{3} + V_3^2 - \frac{2V_1V_2}{3} + V_3V_2 - V_3V_1\right) \quad (1)$$

where C_i is the structure capacitance between two conductor layers and can be expressed as $C_1 = \frac{\varepsilon_r\varepsilon_o h}{d}$,where h and d are the height and separation of the two conductor layers. Also, V_1, V_2 and V_3 are correlate terminal voltages given by $V_1 = -V_2 = \frac{1}{n}V_{winding}, V_3 = 0$ for the conventional multi-layer winding, and $V_1 = V_2 = -V_3 = \frac{1}{n}V_{winding}$ for the fold-back winding, where n is the number of layers and $V_{winding}$ is the voltage across the winding.

The high number of turns and insulation requirements for high-voltage windings lead to transformers having multi-layer windings. Unfortunately, conventional multi-layer windings tend to have higher parasitic capacitances [13], [19]; as a result, special attention must be placed on their configuration. This paper will study three different winding arrangements for the high voltage winding, as seen in Fig. 1. Fig. 1(a) is a convectional multi-layer winding, Fig. 1(b) is a fold-back multi-layer winding, and Fig. 1(c) is a multi-layer multi-section fold-back winding. Fig. 2 shows the conventional winding and triple fold-back windings built for this work. Table I shows the design parameters of the medium-voltage medium-frequency transformer used to study the effect of its stray capacitances.

III. TRANSFORMER IMPEDANCE RESPONSES

Fig. 3 shows the equivalent circuit that take into account stray capacitances on the transformer. Using these model, a vector network analyzer can be used to measure the impedance response of the windings. The impedance response of the three

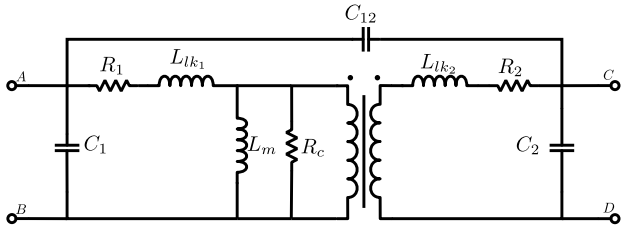

Fig. 3. Transformer parasitic equivalent circuit.

TABLE II
CURRENT RESONANCE FREQUENCIES FOR ALL WINDING ARRANGEMENTS

	Impedance Response Resonance Point	Open-Circuit Resonance Point
Conventional	1.58 MHz	1.76 MHz
Foldback	7.0 MHz	6.74 MHz
Triple Foldback	25 MHz	>10 MHz

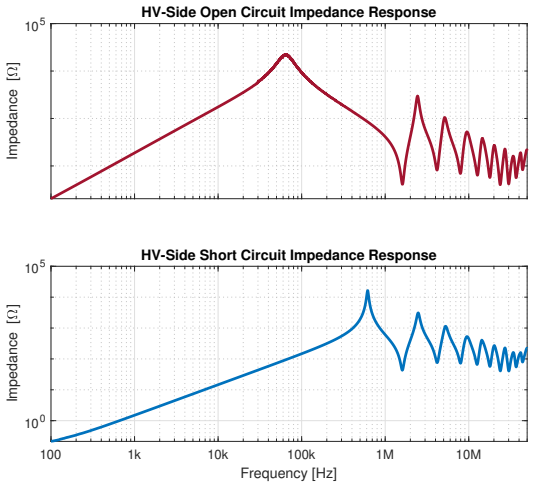

Fig. 4. Open-circuit and short-circuit of conventional winding arrangement.

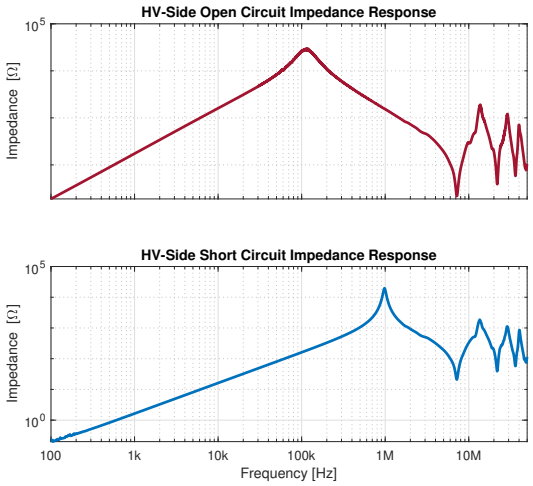

Fig. 5. Open-circuit and short-circuit of fold-back winding arrangement.

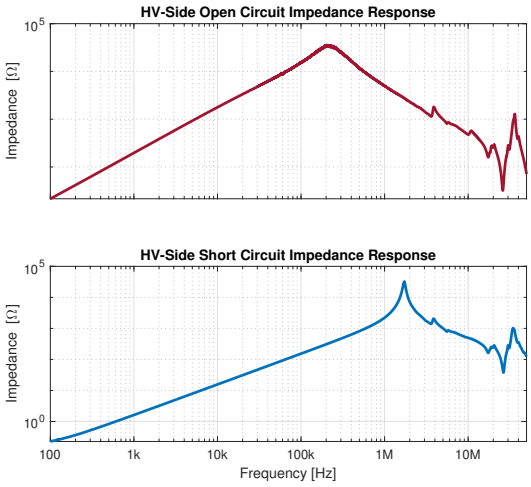

Fig. 6. Open-circuit and short-circuit of triple fold-back winding arrangement.

windings arrangements are measured using Omicron Vector Network Analyzer Bode 100. Fig. 4 shows the open-circuit and short-circuit impedance responses of high-voltage winding where it presented a resonance point of about 1.58 MHz. The impedance response of the fold-back winding is shown in Fig. 5 with a resonance point of about 7 MHz. Finally, the triple fold-back winding showed a resonance point greater than 20 MHz as seen in Fig. 6. From the open-circuit and short-circuit impedance responses summarized in Table II, the splitting of the primary winding can significantly mitigate the parasitic capacitance of the high-voltage winding and move the resonance point to high frequencies.

To compare the diminishing effect upon the parasitic capacitance of the conventional winding arrangement and the split fold-back winding arrangement, the impedance model of the transformer according to [20] can be obtained using the Vector Network Analyzer Bode 100. Table III states the impedances for the conventional winding and the triple fold-back winding. The measurements of the parasitic capacitances of the primary winding for the split fold-back winding showed a reduction by a factor greater than 40 times compared to the conventional winding parasitic capacitances. This result supports one of the open-circuit and short-circuit impedances responses where the resonance frequency for the split fold-back winding is about 20 times higher than that of the conventional winding.

IV. TRANSFORMER CURRENT RESONANCE EXPERIMENTAL RESULTS

A single-phase DAB converter composed of 10-kV SiC MOSFETs on the primary bridge and 1.2 kV SiC MOSFETs on the secondary bridge, whose design is outside the scope of this paper, was used to characterize the medium-frequency transformer. This converter is used to study the parasitic capacitances on the system under no-load and load conditions. An open-circuit or two-winding test was performed from the primary side of the converter using an MSO58 Tektronix scope.

TABLE III
SINGE-PHASE WINDING IMPEDANCE CHARACTERIZATION

Winding	L_m	L_{lk1}	L_{lk2}	C_1	C_2	C_{12}
Conventional	38.787 mH	228.44 μH	4.0 μH	224 pF	4 pF	67.4 pF
Split	39.653 mH	237.7 μH	4.17 μH	5 pF	12 pF	40 pF

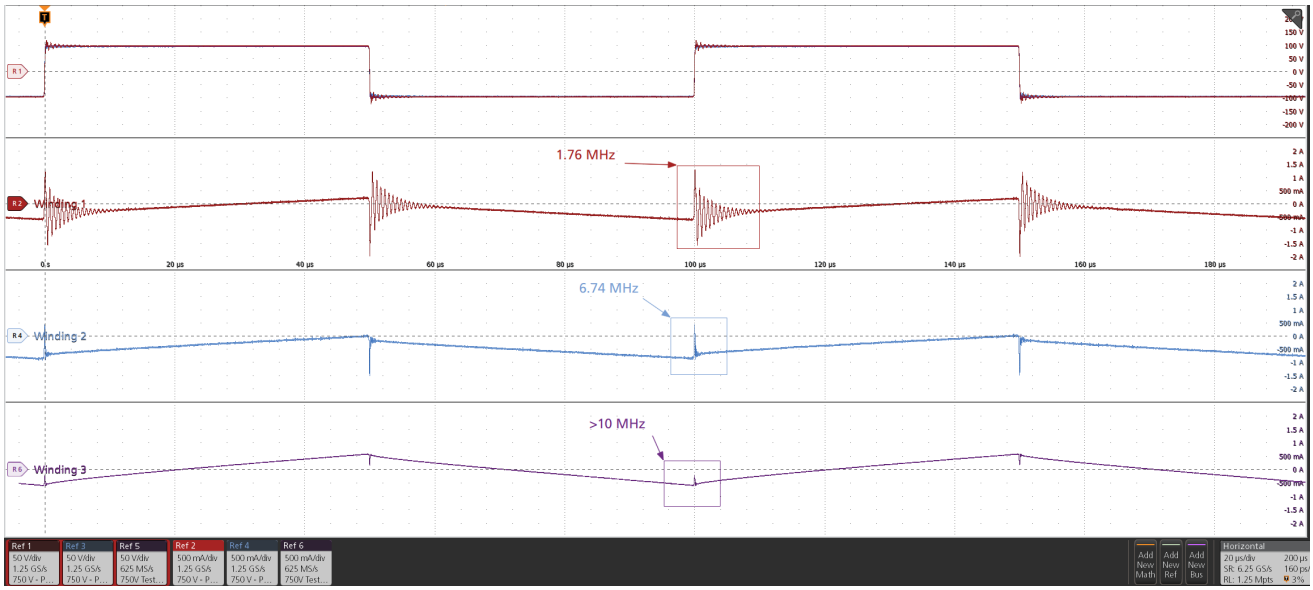

Fig. 7. Considered winding arrangements (a) Conventional multi-layer winding; (b) Fold-back winding; (c) Split fold-back winding.

The current waveforms for each of the winding arrangements are shown in Fig. 7. The current on the conventional winding clearly illustrates the impact of the parasitic capacitances. Furthermore, Fig. 7 exemplifies the mitigation of the current resonances as different winding arrangements are used. The results showed a resonance frequency of 1.76 MHz for the conventional winding current in red while the split fold-back winding current on purple has a resonance frequency above 10 MHz. Furthermore, a 10-kW load test was performed on the conventional winding and triple fold-back winding which are illustrated in Fig. 8. This results showed that the high frequency current resonance occur during the step of the secondary voltage and also it showed the reduction of such resonances as a result of the splitting fold-back of the high-voltage winding.

V. CONCLUSIONS

The experimental results of the high-voltage converter under load conditions showed that stray capacitance present an issue to the overall performance of the converter and attention needs to be paid to the design of high number of turns windings. Open-circuit and short-circuit impedance response showed the improvement of the resonance point as a more complex winding arrangement is used. Triple fold-back winding showed a resonance point 20 times higher than the conventional winding, resulting in the complete mitigation of the current oscillation under no-load and load conditions.

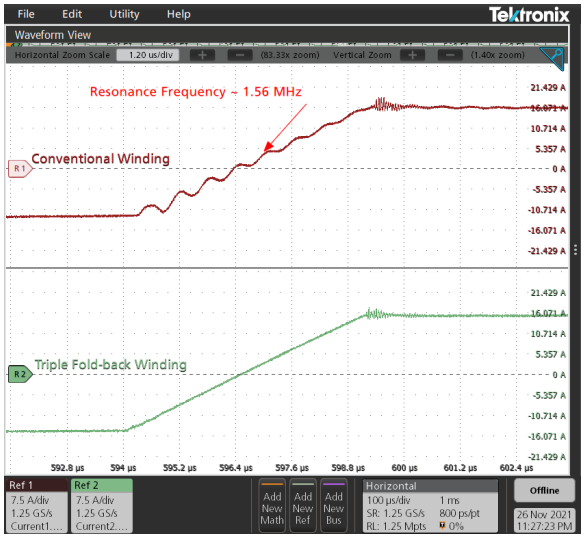

Fig. 8. Current resonance during secondary voltage step-up for a 10-kW load test

REFERENCES

[1] B. Cougo and J. W. Kolar, "Integration of leakage inductance in tape wound core transformers for dual active bridge converters," in *2012 7th International Conference on Integrated Power Electronics Systems (CIPS)*. IEEE, 2012, pp. 1–6.

[2] S. Inoue and H. Akagi, "A bidirectional isolated dc–dc converter as a core circuit of the next-generation medium-voltage power conversion

system," *IEEE Transactions on Power Electronics*, vol. 22, no. 2, pp. 535–542, 2007.

[3] R. W. De Doncker, D. M. Divan, and M. H. Kheraluwala, "A three-phase soft-switched high-power-density dc/dc converter for high-power applications," *IEEE transactions on industry applications*, vol. 27, no. 1, pp. 63–73, 1991.

[4] H. Zhou and A. M. Khambadkone, "Hybrid modulation for dual active bridge bi-directional converter with extended power range for ultracapacitor application," in *2008 IEEE Industry Applications Society Annual Meeting*. IEEE, 2008, pp. 1–8.

[5] M. Kaymak, R. W. De Doncker, and T. Jimichi, "Design and verification of a medium-frequency transformer in a three-phase dual-active bridge dc-dc converter for medium-voltage grid connection of offshore wind farms," in *2020 IEEE Applied Power Electronics Conference and Exposition (APEC)*. IEEE, 2020, pp. 2694–2701.

[6] S. Haghbin, M. Alatalo, F. Yazdani, T. Thiringer, and R. Karlsson, "The design and construction of transformers for a 50 kw three-phase dual active bridge dc/dc converter," in *2017 IEEE Vehicle Power and Propulsion Conference (VPPC)*. IEEE, 2017, pp. 1–5.

[7] W. Shen, *Design of high-density transformers for high-frequency high-power converters*. Ph.D. dissertation, Virginia Polytechnic Institute and State University, 2006.

[8] C. Liu, L. Qi, X. Cui, and X. Wei, "Experimental extraction of parasitic capacitances for high-frequency transformers," *IEEE Transactions on Power Electronics*, vol. 32, no. 6, pp. 4157–4167, 2016.

[9] A. Portolan and I. Hofsajer, "The analysis and design of an inter-winding shielding structure of a high frequency transformer," in *2007 IEEE Power Engineering Society Conference and Exposition in Africa-PowerAfrica*. IEEE, 2007, pp. 1–6.

[10] Z. Qin, Z. Shen, and F. Blaabjerg, "Modelling and analysis of the transformer current resonance in dual active bridge converters," in *2017 IEEE Energy Conversion Congress and Exposition (ECCE)*. IEEE, 2017, pp. 4520–4524.

[11] A. K. Das and B. G. Fernandes, "Study of frequency-dependent parasitics' effects on resonance frequencies of a two-winding medium/high-frequency transformer," in *2020 IEEE International Conference on Power Electronics, Drives and Energy Systems (PEDES)*. IEEE, 2020, pp. 1–6.

[12] C. Buchhagen, C. Reese, L. Hofmann, and H. Däumling, "Determination of a capacitance model for inductive medium voltage transformers," in *PES T&D 2012*. IEEE, 2012, pp. 1–6.

[13] J. Biela and J. W. Kolar, "Using transformer parasitics for resonant converters-a review of the calculation of the stray capacitance of transformers," in *Fourtieth IAS Annual Meeting. Conference Record of the 2005 Industry Applications Conference, 2005.*, vol. 3. IEEE, 2005, pp. 1868–1875.

[14] A. K. Das and B. G. Fernandes, "Synthesis of an equivalent π-model of two-winding transformer and resonance frequency estimation using lumped circuit parameters," in *2019 IEEE Energy Conversion Congress and Exposition (ECCE)*. IEEE, 2019, pp. 3025–3032.

[15] C. Østergaard, C. Kjeldsen, and M. Nymand, "Simple equivalent circuit capacitance model for two-winding transformers," in *2020 IEEE Vehicle Power and Propulsion Conference (VPPC)*. IEEE, 2020, pp. 1–6.

[16] M. A. Saket, N. Shafiei, and M. Ordonez, "Planar transformer winding technique for reduced capacitance in llc power converters," in *2016 IEEE Energy Conversion Congress and Exposition (ECCE)*. IEEE, 2016, pp. 1–6.

[17] S. D. Johnson, A. F. Witulski, and R. W. Erickson, "A comparison of resonant topologies in high voltage dc applications," in *1987 2nd IEEE Applied Power Electronics Conference and Exposition*. IEEE, 1987, pp. 145–156.

[18] E. Laveuve, J.-P. Keradec, and M. Bensoam, "Electrostatic of wound components: analytical results, simulation and experimental validation of the parasitic capacitance," in *Conference Record of the 1991 IEEE Industry Applications Society Annual Meeting*. IEEE, 1991, pp. 1469–1475.

[19] R. Ramachandran, M. Nymand, and J. Nielsen, "Analysis and experimental verification of reducing intra-winding capacitance in a copper foil transformer," in *2020 IEEE Applied Power Electronics Conference and Exposition (APEC)*. IEEE, 2020, pp. 2653–2657.

[20] M. Bitschnau. (2017) Transformer modelling, omicron lab. [Online]. Available: https://www.omicron-lab.com